

This article was downloaded by: [Renmin University of China]

On: 13 October 2013, At: 10:46

Publisher: Taylor & Francis

Informa Ltd Registered in England and Wales Registered Number: 1072954 Registered office: Mortimer House, 37-41 Mortimer Street, London W1T 3JH, UK



Journal of Coordination Chemistry

Publication details, including instructions for authors and subscription information:

<http://www.tandfonline.com/loi/gcoo20>

Ferrocene-carboxylate coordination complexes bridged by different N-containing ligands

Jinpeng Li^{a,b}, Huan Sun^a, Qinqin Yuan^a, Xiaoli Gao^a, Shaomin Wang^a, Yanyan Zhu^a, Lu Liu^a, Songhe Zhang^a, Yanan Zhang^a, Yuexin Guo^c, Baoxian Ye^a, Yaru Liu^d, Hongwei Hou^a, Yaoting Fan^a & Junbiao Chang^{a,b}

^a Department of Chemistry, Zhengzhou University, Henan, P.R. China

^b School of Pharmaceutical Sciences, Zhengzhou University, Henan, P.R. China

^c Department of Pharmacy, North China Coal Medicine University, Tangshan, P.R. China

^d School of Science, North University of China, Taiyuan, P.R. China

Accepted author version posted online: 22 Mar 2013. Published online: 29 Apr 2013.

To cite this article: Jinpeng Li, Huan Sun, Qinqin Yuan, Xiaoli Gao, Shaomin Wang, Yanyan Zhu, Lu Liu, Songhe Zhang, Yanan Zhang, Yuexin Guo, Baoxian Ye, Yaru Liu, Hongwei Hou, Yaoting Fan & Junbiao Chang (2013) Ferrocene-carboxylate coordination complexes bridged by different N-containing ligands, *Journal of Coordination Chemistry*, 66:10, 1686-1699, DOI: [10.1080/00958972.2013.788155](https://doi.org/10.1080/00958972.2013.788155)

To link to this article: <http://dx.doi.org/10.1080/00958972.2013.788155>

PLEASE SCROLL DOWN FOR ARTICLE

Taylor & Francis makes every effort to ensure the accuracy of all the information (the "Content") contained in the publications on our platform. However, Taylor & Francis, our agents, and our licensors make no representations or warranties whatsoever as to the accuracy, completeness, or suitability for any purpose of the Content. Any opinions and views expressed in this publication are the opinions and views of the authors, and are not the views of or endorsed by Taylor & Francis. The accuracy of the Content should not be relied upon and should be independently verified with primary sources of information. Taylor and Francis shall not be liable for any losses, actions, claims,

proceedings, demands, costs, expenses, damages, and other liabilities whatsoever or howsoever caused arising directly or indirectly in connection with, in relation to or arising out of the use of the Content.

This article may be used for research, teaching, and private study purposes. Any substantial or systematic reproduction, redistribution, reselling, loan, sub-licensing, systematic supply, or distribution in any form to anyone is expressly forbidden. Terms & Conditions of access and use can be found at <http://www.tandfonline.com/page/terms-and-conditions>

Ferrocene-carboxylate coordination complexes bridged by different N-containing ligands

JINPENG LI†‡, HUAN SUN†, QINQIN YUAN†, XIAOLI GAO†, SHAOMIN WANG†, YANYAN ZHU†, LU LIU†, SONGHE ZHANG†, YANAN ZHANG†, YUEXIN GUO§, BAOXIAN YE†, YARU LIU¶, HONGWEI HOU†*, YAOTING FAN† and JUNBIAO CHANG†‡*

†Department of Chemistry, Zhengzhou University, Henan, P.R. China

‡School of Pharmaceutical Sciences, Zhengzhou University, Henan, P.R. China

§Department of Pharmacy, North China Coal Medicine University, Tangshan, P.R. China

¶School of Science, North University of China, Taiyuan, P.R. China

(Received 10 October 2012; in final form 17 January 2013)

Six new coordination complexes, $[\text{Cd}(\eta^2\text{-OOCCH}=(\text{CH}_3)\text{Cfc})_2(\text{bix})]_2 \cdot (\text{CH}_3\text{OH})_{0.5}$ (**1**), $[\text{Zn}(\eta^2\text{-OOCCH}=(\text{CH}_3)\text{Cfc})(\eta^1\text{-OOCCH}=(\text{CH}_3)\text{Cfc})(\text{bix})]_2 \cdot (\text{H}_2\text{O})_{0.5}$ (**2**), $[\text{Zn}(\eta^2\text{-OOCCH}=(\text{CH}_3)\text{Cfc})_2(\text{pbbm})]_2 \cdot (\text{CH}_3\text{OH})_2$ (**3**), $\{[\text{Mn}(\eta^1\text{-OOCCH}=(\text{CH}_3)\text{Cfc})_2(\text{bbbm})(\text{H}_2\text{O})_2] \cdot (\text{CH}_3\text{OH})_3\}_n$ (**4**), $\{[\text{Cd}(\eta^1\text{-OOCCH}=(\text{CH}_3)\text{Cfc})_2(\text{pbbm})] \cdot (\text{CH}_3\text{OH})_2\}_n$ (**5**), and $[\text{Cd}(\eta^2\text{-OOCCH}=(\text{CH}_3)\text{Cfc})_2(\text{pmbbm})]_n$ (**6**) $\{\text{Fc}=(\eta^5\text{-C}_5\text{H}_4)\text{Fe}(\eta^5\text{-C}_5\text{H}_4)\}$, $\text{bix}=1,4\text{-bis}(\text{imidazol-1-ylmethyl})\text{benzene}$, $\text{pbbm}=1,1'\text{-}[(1,4\text{-propanediyl})\text{bis-1H-benzimidazole}]$, $\text{bbbm}=1,1'\text{-}[(1,4\text{-butanediyl})\text{bis-1H-benzimidazole}]$, $\text{pmbbm}=1,1'\text{-}[(1,4\text{-pentanediyl})\text{bis-1H-benzimidazole}]$, were prepared and characterized. X-ray crystallographic analysis reveals that **1–3** are dimers bridged by bix and pbbm . Complexes **4–6** are one-dimensional (1-D) structures bridged by bbbm and pmbbm , respectively. Various $\pi\text{-}\pi$ interactions were discovered in **1–6** that make significant contributions to molecular self-assembly. Solution differential pulse voltammetry of **1–6** indicates that the half-wave potentials of the ferrocenyl moieties in these complexes shift to positive potential compared with that of 3-ferrocenyl-2-crotonic acid.

Keywords: Ferrocene-carboxylate; Nitrogen heterocyclic; Crystal structure; Electrochemistry

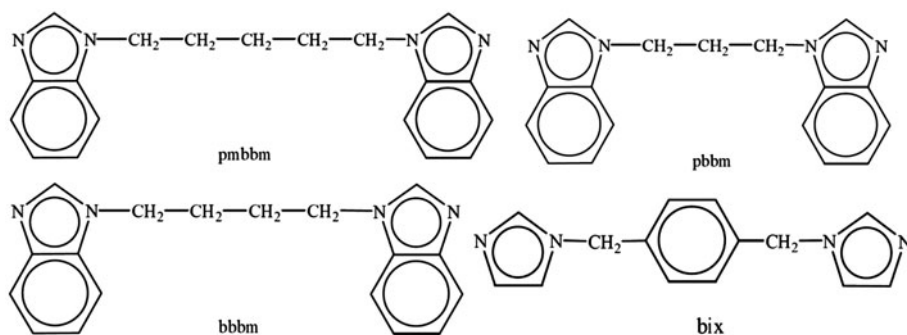
1. Introduction

Design and construction of metal-organic complexes have experienced growth due to their fascinating structures [1] and potential applications in catalysis, luminescence, gas storage, ion exchange, etc. [2–4]. A number of complexes with multiple structures and interesting properties have been synthesized and reported [5, 6]. However, it is still a challenge to control the structures and compositions of desired metal-organic complexes, because the self-assembly process is influenced by many factors such as the nature of the ligands, the inorganic anions, metal/ligand ratio, solvent media, etc. [7–10]. The ligand is crucial and usually the first choice for designing coordination complexes, since it can adjust the coordination modes, flexibility of the molecular backbone, configurational preference, type,

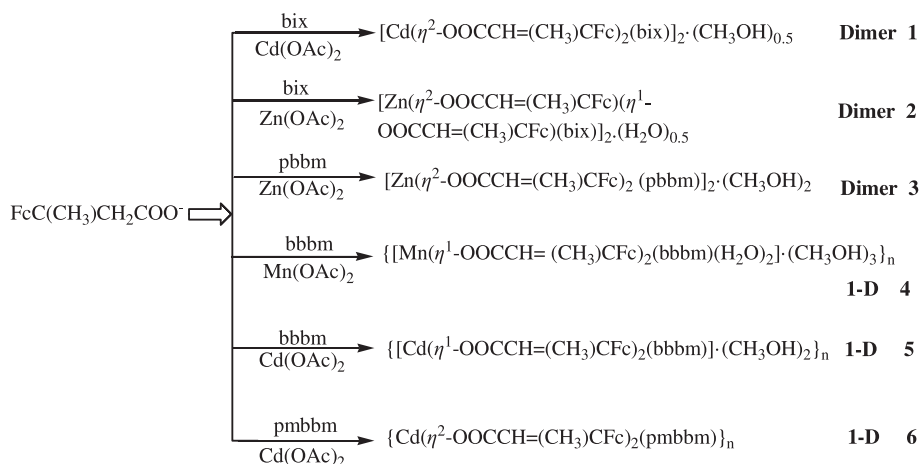
*Corresponding authors. Email: houghongw@zzu.edu.cn (H. Hou); changjunbiao@zzu.edu.cn (J. Chang)

and topology of the products by coordinating directly to metal centers [11]. The fascinating stereochemical and electrochemical properties of ferrocene [12] derivatives have attracted attention [13–15], and a series of ligands containing ferrocene have been reported [16, 17]. Coordinating capability of carboxylates to metal ions is strong and the coordination modes are versatile [18–20]. Therefore, it is a good choice to utilize ferrocenyl carboxylates as ligands to synthesize functional complexes. Flexible nitrogen-heterocyclic ligands containing imidazole, triazole, and their derivatives can freely bend or rotate to meet the requirement of coordination geometries, often used as adjuvant ligands to construct complexes. Their aromatic rings attract our interest because of potential strong π - π stacking interactions [21, 22].

As an extension of our earlier studies, a series of nitrogen-heterocyclic ligands (scheme 1) and 3-ferrocenyl-2-crotonic acid were chosen to react with metal salts. Herein, we report the preparations and crystal structures of six new coordination complexes (scheme 2) assembled by π - π stacking interactions and weak hydrogen bonds in combination with metal-ligand bonds. Electrochemical properties were also investigated.



Scheme 1. Nitrogen-heterocyclic ligands.



Scheme 2. Syntheses of 1–6.

2. Experimental

2.1. General information and materials

3-Ferrocenyl-2-crotonic acid [23], 1,1'-[(1,4-pentanediy)bis-1H-benzimidazole] (pbbm), 1,1'-[(1,4-butanediyl)bis-1H-benzimidazole] (bbbm), 1,1'-[(1,4-propanediyl)bis-1H-benzimidazole] (pbbm), and 1,4-[bis(imidazol-1-ylmethyl)benzene] (bix) were prepared by literature methods [24]. All other chemicals were reagent grade quality obtained from commercial sources and used without purification. Carbon, hydrogen, and nitrogen analyses were carried out on a FLASH EA 1112 elemental analyzer. IR data were recorded on a BRUKER TENSOR 27 spectrophotometer with KBr pellets from 400 to 4000 cm^{-1} . ^1H NMR spectra were recorded on a BRUKER AM-300 spectrometer at room temperature in DMSO. Cyclic voltammetric experiments were performed by employing a CHI660B electrochemical analyzer. A three-electrode system was used, consisting of a platinum working electrode, a platinum wire auxiliary electrode, and a Hg/HgCl₂ reference electrode. The measurements were carried out in DMF with tetrabutyl ammonium perchlorate (*n*-Bu₄NClO₄) (0.10 M dm⁻³) as a supporting electrolyte. To prevent fouling, the working electrode was polished.

2.2. Preparation of [Cd(η^2 -OOCCH=(CH₃)CFc)₂(bix)]₂·(CH₃OH)_{0.5} (1)

A methanol solution (4 mL) of bix (12.0 mg, 0.05 mM) was added to a methanol solution (6 mL) of Cd(OAc)₂·2H₂O (13.4 mg, 0.05 mM), and then, a methanol solution (4 mL) of NaOOCCH=C(CH₃)Fc (29.2 mg, 0.10 mM) was added dropwise into the mixture. The resultant solution was kept at room temperature. Red crystals suitable for X-ray diffraction were formed three weeks later. Yield: 47%. Anal. Calcd for C_{84.5}H₈₀Cd₂Fe₄N₈O_{8.5}: C, 56.81; H, 4.51; N, 6.315%. Found: C, 55.62; H, 4.47; N, 6.48%. IR (cm^{-1} , KBr): 3431 m, 2382 w, 1620 s, 1527 s, 1402 m, 1385 m, 1333 w, 1255 w, 1109 m, 1087 w, 1030 w, 939 w, 821 m, 749 w, 654 w, 498 w. ^1H NMR (400 M L⁻¹, DMSO): δ = 7.90 (s, 1H), 7.22 (d, 2H), 6.90 (s, 1H), 6.03 (s, 1H), 5.18 (s, 2H), 4.55 (t, 2H), 4.33 (t, 2H), 4.13 (s, 5H), 2.49 (m, 3H).

2.3. Preparation of [Zn(η^2 -OOCCH=(CH₃)CFc)(η^1 -OOCCH=(CH₃)CFc)(bix)]₂(H₂O)_{0.5} (2)

The procedure was the same as that for **1**, Zn(OAc)₂·2H₂O (11.0 mg, 0.05 mM) was used instead of Cd(OAc)₂·2H₂O (13.4 mg, 0.05 mM). Yield: 46%. Anal. Calcd for C₈₄H₈₀Fe₄N₈O_{8.5}Zn₂: C, 55.87; H, 4.50; N, 12.45%. Found: C, 55.60; H, 4.44; N, 12.23%. IR (cm^{-1} , KBr): 3422 w, 3131 w, 1624 s, 1585 s, 1378 s, 1325 w, 1297 s, 1204 s, 1118 w, 1090 s, 999 s, 949 s, 931 w, 873 w, 820 s, 761 s, 671 s, 657 w, 621 s, 508 s. ^1H NMR (400 M L⁻¹, DMSO): δ = 8.02 (s, 1H), 7.27 (s, 3H), 7.03 (s, 1H), 5.99 (s, 1H), 5.23 (s, 2H), 4.53 (s, 2H), 4.32 (t, 2H), 4.13 (s, 5H), 2.44 (d, 3H).

2.4. Preparation of [Zn(η^2 -OOCCH=(CH₃)CFc)₂(pbbm)]₂·(CH₃OH)₂ (3)

The procedure was the same as that for **2**, pbbm was used instead of bix. Yield: 51%. Anal. Calcd for C₄₆H₄₁Fe₂N₄O₅Zn: C, 60.87; H, 4.52; N, 6.17%. Found: C, 60.63; H, 4.47; N, 6.33%. IR (cm^{-1} , KBr): 3420 m, 3095 m, 1618 s, 1558 s, 1520 m, 1466 m, 1385 s,

1253s, 1103w, 751s, 498 m. ^1H NMR (400 M L $^{-1}$, DMSO): δ =8.45 (s, 1H), 7.77 (d, 1H), 7.63 (d, 1H), 7.26 (m, 2H), 6.03 (s, 1H), 4.53 (d, 2H), 4.35 (m, 4H), 4.12 (s, 5H), 2.49 (d, 3H), 2.35 (d, 1H).

2.5. Preparation of $\{[\text{Mn}(\eta^1\text{-OOCCH}=\text{C}(\text{CH}_3)\text{Fc})_2(\text{bbbm})(\text{H}_2\text{O})_2]\cdot(\text{CH}_3\text{OH})_3\}_n$ (**4**)

A methanol solution (5 mL) of NaOOCCH=C(CH₃)Fc (29.2 mg, 0.10 mM) was added to a methanol solution (5 mL) of Mn(OAc)₂·2H₂O (12.9 mg, 0.05 mM), and then, a methanol solution (6 mL) of bbbm (30.4 mg, 0.10 mM) was added to the above mixture. The resulting mixture was kept at room temperature in the dark. Two weeks later, red crystals suitable for X-ray diffraction were obtained from the resultant orange solution. Yield: 48%. Attention: the crystal was not stable in the air. Anal. Calcd for C₄₉H₆₀Fe₂MnN₄O₉: C, 57.89; H, 5.91; N, 5.51%. Found: C, 57.77; H, 5.87; N, 5.66%. IR (cm $^{-1}$, KBr): 3633w, 3299w, 1617s, 1531s, 1503s, 1460w, 1406s, 1387s, 1334w, 1289s, 1257s, 1201s, 1105w, 936s, 822s, 748s, 639w, 471s, 426s.

2.6. Preparation of $\{[\text{Cd}(\eta^1\text{-OOCCH}=(\text{CH}_3)\text{CFc})_2(\text{bbbm})]\cdot(\text{CH}_3\text{OH})_2\}_n$ (**5**)

The procedure was the same as that for **4**, Cd(OAc)₂·2H₂O (13.4 mg, 0.05 mM) was used instead of Mn(OAc)₂·H₂O (12.9 mg, 0.05 mM). Yield: 50%. Anal. Calcd for C₅₀H₆₀CdFe₂N₄O₈: C, 57.71; H, 5.61; N, 5.24%. Found: C, 57.52; H, 5.55; N, 5.43%. IR (cm $^{-1}$, KBr): 3638w, 3441 m, 1618s, 1532s, 1506 m, 1460 m, 1386s, 1334 m, 1258 m, 1201 m, 1104 m, 823w, 750s, 495 m. ^1H NMR (400 M L $^{-1}$, DMSO): δ =8.24 (s, 1H), 7.64 (t, 3H), 7.58 (t, 1H), 7.22 (m, 2H), 6.02 (d, 1H), 4.56 (s, 2H), 4.37 (m, 2H), 4.24 (s, 1H), 4.12 (s, 5H), 2.47 (m, 3H), 1.75 (s, 2H).

2.7. Preparation of $[\text{Cd}(\eta^2\text{-OOCCH}=(\text{CH}_3)\text{CFc})_2(\text{pmbbm})]_n$ (**6**)

The procedure was the same as that for **5**, pmbbm (31.8 mg, 0.10 mM) was used instead of bbbm (30.4 mg, 0.10 mM). Yield: 45%. Anal. Calcd for C₄₈H₅₀CdFe₂N₄O₅: C, 58.36; H, 5.07; N, 5.67%. Found: C, 58.18; H, 5.17; N, 5.79%. IR (cm $^{-1}$, KBr): 3429 m, 3097 m, 1618s, 1527s, 1461 m, 1406s, 1294 m, 1255 m, 1105w, 826w, 744s, 498 m. ^1H NMR (400 M L $^{-1}$, DMSO): δ =8.25 (s, 1H), 7.68 (t, 3H), 7.60 (t, 1H), 7.21 (m, 2H), 6.03 (d, 1H), 4.59 (s, 2H), 4.39 (m, 2H), 4.25 (s, 1H), 4.17 (s, 5H), 2.45 (m, 3H), 1.79 (s, 3H).

2.8. Crystallographic studies

The diffraction intensity data of **1–6** were measured at room temperature on a Rigaku RAXIS-IV diffractometer using graphite monochromated Mo- $K\alpha$ radiation (λ =0.71073 Å). The structures were solved by direct methods and expanded with Fourier techniques. The non-hydrogen atoms were refined anisotropically. Hydrogens were included but not refined. The final cycle of full-matrix least-squares refinement was based on observed reflections and variable parameters. All calculations were performed with the SHELXL-97 crystallographic software package [25]. Tables 1 and 2 show crystallographic crystal data and processing parameters for all complexes, and table 3 lists selected bond lengths and angles.

Table 1. Crystallographic data for 1–3.

Complexes	1	2	3
Formula	C _{84.50} H ₈₀ Cd ₂ Fe ₄ N ₈ O _{8.5}	C ₈₄ H ₈₀ Fe ₄ N ₈ O _{8.5} Zn	C ₄₆ H ₄₁ Fe ₂ N ₄ O ₅ Zn
fw	1791.77	1691.70	906.90
Temperature (K)	293(2)	293(2)	293(2)
Wavelength (Å)	0.71073	0.71073	0.71073
Crystal system	Monoclinic	Monoclinic	Triclinic
Space group	<i>P2(1)/c</i>	<i>P2(1)/c</i>	<i>Pī</i>
<i>a</i> (Å)	13.695(3)	13.634(3)	12.410(3)
<i>b</i> (Å)	22.822(5)	22.783(5)	14.684(3)
<i>c</i> (Å)	13.367(3)	13.373(3)	14.987(3)
<i>α</i> (deg)	90	90	89.81(3)
<i>β</i> (deg)	107.98(3)	108.89(3)	74.62(3)
<i>γ</i> (deg)	90	90	78.16(3)
<i>V</i> (Å ³)	3973.7(14)	3930.1(14)	2573.4(9)
<i>Z</i>	2	2	2
<i>D_c</i> (g cm ⁻³)	1.497	1.430	1.170
<i>F</i> (000)	1822	1744	934
<i>θ</i> range for data collection (deg)	3.10–27.42	3.09–27.47	2.47–25.00
Reflections collected/unique	46,637/9047	46,726/8896	25,833/9048
Data/restraints/parameters	9047/0/493	8896/80/481	9048/64/542
Goodness-of-fit on <i>F</i> ²	1.005	0.978	0.926
Final <i>R</i> ₁ ^a , <i>wR</i> ₂ ^b	0.0776, 0.1723	0.0578, 0.1476	0.0794, 0.2347

^a*R*₁ = $\frac{\sum |F_o| - \sum |F_c|}{\sum |F_o|}$. ^b*wR*₂ = $[\sum w(|F_o|^2 - |F_c|^2)^2 / \sum w|F_o|^2]^2$. $w = 1/[\sigma^2(F_o)^2 + 0.0297P^2 + 27.5680P]$, where $P = (F_o^2 + 2F_c^2)/3$.

Table 2. Crystallographic data for 4–6.

Complexes	4	5	6
Formula	C ₄₉ H ₆₀ Fe ₂ MnN ₄ O ₉	C ₅₀ H ₆₀ CdFe ₂ N ₄ O ₈	C ₄₈ H ₅₀ CdFe ₂ N ₄ O ₅
fw	1015.65	1069.13	987.02
Temperature (K)	293(2)	293(2)	293(2)
Wavelength (Å)	0.71073	0.71073	0.71073
Crystal system	Triclinic	Triclinic	Triclinic
Space group	<i>Pī</i>	<i>Pī</i>	<i>Pī</i>
<i>a</i> (Å)	8.8641(18)	8.3825(17)	10.507(2)
<i>b</i> (Å)	9.5992(19)	9.6734(19)	11.567(2)
<i>c</i> (Å)	15.267(3)	15.261(3)	19.424(4)
<i>α</i> (deg)	89.42(3)	85.77(3)	92.96(3)
<i>β</i> (deg)	73.37(3)	74.76(3)	101.48(3)
<i>γ</i> (deg)	79.07(3)	81.64(3)	109.93(3)
<i>V</i> (Å ³)	1220.8(4)	1180.4(4)	2156.6(7)
<i>Z</i>	1	1	2
<i>D_c</i> (g cm ⁻³)	1.382	1.504	1.520
<i>F</i> (000)	531	552	1012
<i>θ</i> range for data collection (deg)	3.13–25.00	3.08–27.50	3.24–27.47
Reflections collected/unique	12,496/4299	14,381/5375	25,894/9758
Data/restraints/parameters	4299/0/307	5375/0/319	9758/34/545
Goodness-of-fit on <i>F</i> ²	1.082	1.061	1.109
Final <i>R</i> ₁ ^a , <i>wR</i> ₂ ^b	0.0599, 0.1573	0.0423, 0.0973	0.0544, 0.1397

^a*R*₁ = $\frac{\sum |F_o| - \sum |F_c|}{\sum |F_o|}$. ^b*wR*₂ = $[\sum w(|F_o|^2 - |F_c|^2)^2 / \sum w|F_o|^2]^2$. $w = 1/[\sigma^2(F_o)^2 + 0.0297P^2 + 27.5680P]$, where $P = (F_o^2 + 2F_c^2)/3$.

Table 3. Selected bond lengths (Å) and angles (deg) for 1–6.

Complex 1					
Cd(1)–N(4)	2.219(6)	Cd(1)–N(1)	2.251(6)	Cd(1)–O(6)	2.297(5)
Cd(1)–O(3)	2.361(6)	Cd(1)–O(4)	2.425(5)	Cd(1)–O(1)	2.245(3)
N(4)–Cd(1)–N(1)	117.6(2)	N(4)–Cd(1)–O(6)	98.9(2)	N(1)–Cd(1)–O(6)	124.5(2)
Complex 2					
Zn(1)–O(4)	1.993(4)	Zn(1)–O(2)	1.994(4)	Zn(1)–N(3)	2.023(4)
Zn(1)–N(1)	2.026(4)	O(4)–Zn(1)–O(2)	116.96(19)	O(4)–Zn(1)–N(3)	92.34(17)
O(2)–Zn(1)–N(3)	109.28(17)	O(4)–Zn(1)–N(1)	104.41(18)	O(2)–Zn(1)–N(1)	116.08(18)
Complex 3					
Zn(1)–O(1)	1.972(5)	Zn(1)–O(3)	1.999(4)	Zn(1)–N(2)#1	2.035(5)
Zn(1)–N(3)	2.073(5)	O(1)–Zn(1)–O(3)	112.2(2)	O(1)–Zn(1)–N(2)#1	130.7(2)
O(3)–Zn(1)–N(2)#1	105.9(2)	O(1)–Zn(1)–N(3)	101.1(2)	O(3)–Zn(1)–N(3)	104.17(19)
Complex 4					
Mn(1)–O(2)	2.160(3)	Mn(1)–O(2)#1	2.160(3)	Mn(1)–O(1)#1	2.220(3)
Mn(1)–O(1)	2.220(3)	Mn(1)–N(1)#1	2.260(3)	Mn(1)–N(1)	2.260(3)
O(2)–Mn(1)–O(2)#1	180.0	O(2)–Mn(1)–O(1)#1	89.85(12)	O(2)–Mn(1)–O(1)	90.15(12)
O(2)#1–Mn(1)–O(1)#1	90.15(12)	O(2)#1–Mn(1)–O(1)	89.85(12)	O(1)#1–Mn(1)–O(1)	180.0
Complex 5					
Cd(1)–O(2)#	2.262(2)	Cd(1)–O(2)	2.262(2)	Cd(1)–N(1)#1	2.325(2)
Cd(1)–N(1)	2.325(2)	Cd(1)–O(5)#1	2.381(2)	N(1)–Cd(1)–O(5)#1	87.15(9)
O(2)#1–Cd(1)–O(2)	180.0	O(2)#1–Cd(1)–N(1)#1	87.64(9)	O(2)–Cd(1)–N(1)#1	92.36(9)
O(2)#1–Cd(1)–N(1)	92.36(9)	O(2)–Cd(1)–N(1)	87.64(9)	N(1)#1–Cd(1)–N(1)	180.0
Complex 6					
Cd(1)–N(3)	2.291(3)	Cd(1)–O(3)	2.311(3)	Cd(1)–N(1)#1	1.469(5)
Cd(1)–O(1)	2.385(3)	Cd(1)–O(4)	2.351(3)	O(3)–Cd(1)–O(1)	117.68(12)
N(3)–Cd(1)–O(4)	84.84(12)	N(2)–Cd(1)–O(4)	104.83(13)	O(3)–Cd(1)–O(4)	55.50(9)
N(3)–Cd(1)–O(2)	96.31(14)	N(2)–Cd(1)–O(2)	137.63(13)	O(3)–Cd(1)–O(2)	98.20(9)

Symmetry transformations used to generate equivalent atoms: For 1: #1 $-x, -y+1, -z+1$; #2 $-x+1, -y+1, -z+1$. For 2: #1 $-x, -y+1, z+1$. For 3: #1 $-x+1, -y+1, -z$. For 4: #1 $-x+1, -y+1, -z$, #2 $-x+2, -y+2, -z$. For 5: #1 $-x+1, -y+1, -z$; #2 $-x+2, -y+2, -z$. For 6: #1 $x-1, y-1, z$; #2 $x+1, y+1, z$.

3. Results and discussion

3.1. Crystal structures of $[\text{Cd}(\eta^2\text{-OOCCH}=(\text{CH}_3)\text{Cfc})_2(\text{bix})]_2 \cdot (\text{CH}_3\text{OH})_{0.5} (\mathbf{1})$, $\{\text{Zn}(\eta^2\text{-OOCCH}=(\text{CH}_3)\text{Cfc})(\eta^1\text{-OOCCH}=(\text{CH}_3)\text{Cfc})(\text{bix})\}_2 \cdot (\text{H}_2\text{O})_{0.5} (\mathbf{2})$, and $[\text{Zn}(\eta^2\text{-OOCCH}=(\text{CH}_3)\text{Cfc})_2(\text{pbbm})]_2 \cdot (\text{CH}_3\text{OH})_2 (\mathbf{3})$

X-ray diffraction analyses reveal that **1** and **2** crystallize in the monoclinic space group $P2_1(1)/c$ and exhibit similar dimeric structures. Each Cd(II) in **1** is six-coordinate in a distorted octahedron, defined by four oxygens (O3, O4, O5, O6) from two symmetry-related $\eta^2\text{-OOCCH}=(\text{CH}_3)\text{Cfc}$ groups and two nitrogens (N1, N4) from two independent *cis* bix (figure 1). The bond angles between the six donating atoms are 53.66(19)–173.8(2)°, deviating severely from an ideal octahedron. The Cd···Cd separation is 11.5328(3) Å. Cd–N lengths are 2.219(6) and 2.251(6) Å, shorter than the Cd–O lengths [2.297(5)–2.491(6) Å]. The results correspond to those of other Cd complexes having a distorted octahedral environment, such as $[\text{Cd}(\text{en})(\text{NO}_3)_2(4,4'\text{-bpy})]_n$ [en = ethylenediamine, Cd–N: 2.354(2) Å, Cd–O: 2.520(2) Å] [26]. In **2** (figure 2), each Zn(II) is best portrayed as an axially distorted, trigonal bipyramidal geometry ligated by three oxygens (O1, O2, O4) from two $\text{FcC}(\text{CH}_3)=\text{CHCOO}^-$ anions with different coordination modes, one $\eta^1\text{-}$, the other $\eta^2\text{-}$ mode, and

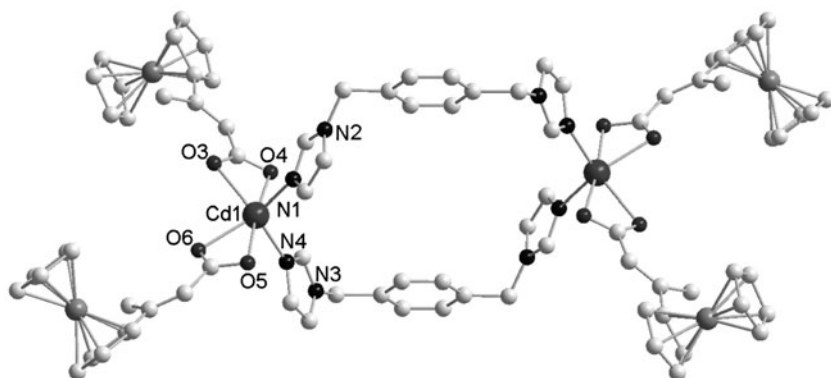


Figure 1. Perspective view with partial atom-labeling scheme of the binuclear structure of $[\text{Cd}(\eta^2\text{-OOCCH}=(\text{CH}_3)\text{CFc})_2(\text{bix})]_2 \cdot (\text{CH}_3\text{OH})_{0.5}$ (**1**).

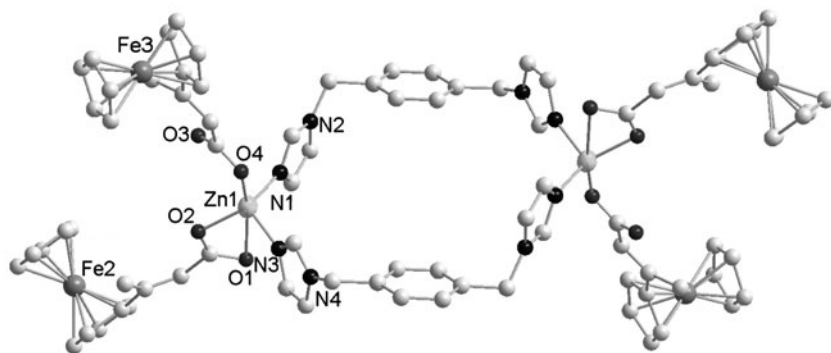


Figure 2. Perspective view with partial atom-labeling scheme of the binuclear structure of $[\text{Zn}(\eta^2\text{-OOCCH}=(\text{CH}_3)\text{CFc})(\eta^1\text{-OOCCH}=(\text{CH}_3)\text{CFc})(\text{bix})]_2 \cdot (\text{H}_2\text{O})_{0.5}$ (**2**).

two nitrogens (N1, N4) from two *cis* bix. The bond angles around Zn(II) vary from 92.34 (17) to 116.96(19)°. Along the axial direction, the angle of $\text{O1} \cdots \text{Zn1} \cdots \text{O4}$ is 170.17(6)°. The Zn–N bond lengths vary from 2.023(4) to 2.026(4) Å, while Zn–O bond lengths are from 1.993(4) to 1.994(4) Å, in the normal range [27]. **1** and **2** have the same aromatic rings, and between the rings, there are similar π – π and CH/ π stacking interactions. Therefore, we only describe **1** in detail. Analysis of the crystal packing of **1** reveals head-to-tail π – π stacking interactions between adjacent imidazole rings of bix with the inter-planar separation of 3.63 Å (center-to-center separation: 3.95 Å) extending the dimers to 2-D layers (figure 3). These 2-D layers are further connected to 3-D supramolecular networks (figure 4) by edge-to-face CH/ π interactions: one is 2.80 Å (dihedral angle: 106.3°, H/ π -plane separation: 2.66 Å) between the adjacent benzene ring and imidazole ring of bix; another is 2.90 Å (dihedral angle 105.2°, H/ π -plane separation: 2.75 Å) between the ferrocene ring and imidazole ring of bix; the other is 2.79 Å (dihedral angle: 81.8°, H/ π -plane separation: 2.74 Å) between adjacent benzene ring of bix and ferrocene ring.

Complex **3** crystallizes in the triclinic space group *P*-1. Each Zn(II) (figure 5) is distorted octahedral via coordination with four oxygens (O1, O2, O3, O4) from two symmetry-related η^2 -OOCCH=(CH₃)CFc moieties and two nitrogens (N2, N3) from two *cis* pbbm. The Zn–N

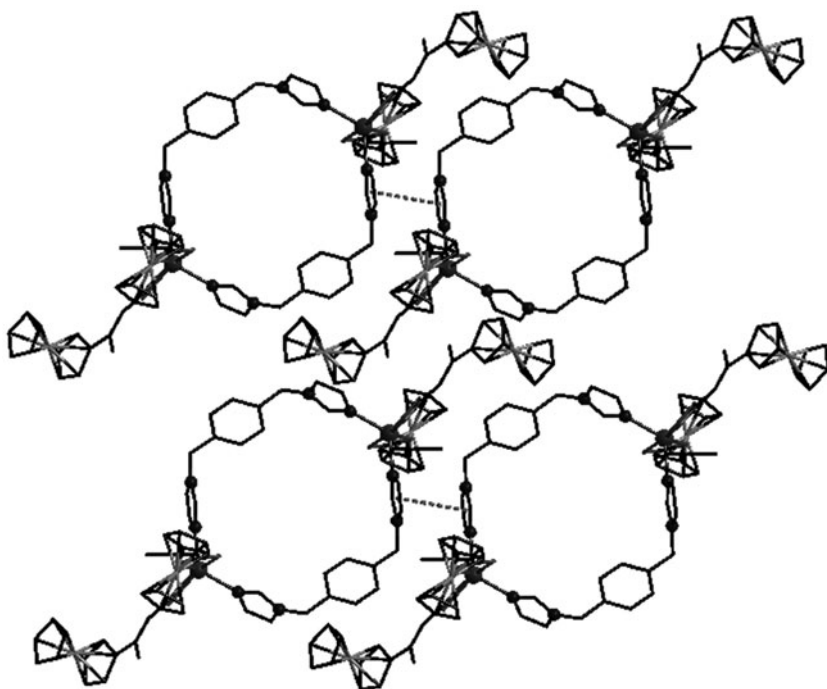


Figure 3. 2-D layered supramolecular network of **1**. The dashed lines represent π - π stacking interactions between two adjacent imidazole rings.

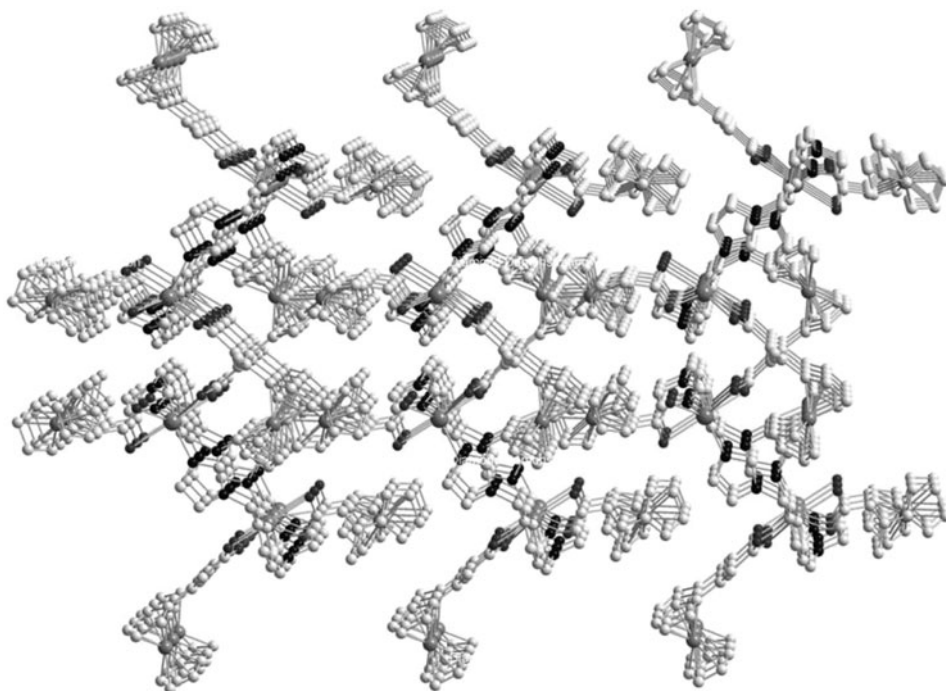


Figure 4. 3-D worm-like supramolecular network of **1**. Hydrogens are omitted for clarity.

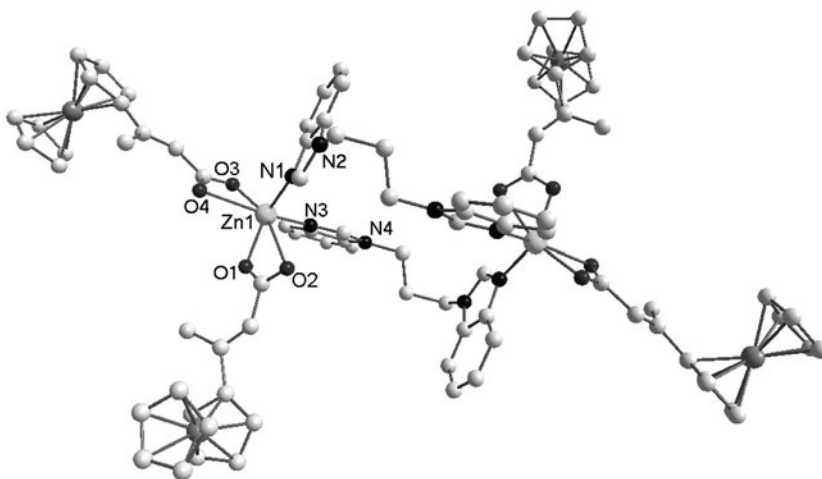


Figure 5. Perspective view with partial atom-labeling scheme of the binuclear structure of $[\text{Zn}(\eta^2\text{-OOCCH}=(\text{CH}_3)\text{CFc})_2(\text{pbbm})]_2 \cdot (\text{CH}_3\text{OH})_2$ (**3**).

bond lengths vary from 2.035(5)–2.073(5) Å, longer than the Zn–O lengths [1.972(5)–1.999(4) Å], consistent with those of **2**. The Zn···Zn distance is 9.493 Å, much shorter than the corresponding value for **2** (11.487 Å), as a result of different bridging nitrogen-heterocyclic ligands. There are π – π stacking interactions in **3** with inter-planar separations of 3.41 Å (center-to-center separations: 3.78 Å) between inter-molecular benzimidazole rings of pbbm. Also, edge-to-face CH/ π interactions are present with 2.92 Å (dihedral angle: 80.4°, H/ π -plane separation: 2.85 Å) between benzimidazole rings and ferrocene rings.

3.2. Crystal structures of $\{[\text{Mn}(\eta^1\text{-OOCCH}=(\text{CH}_3)\text{CFc})_2(\text{bbbm})(\text{H}_2\text{O})_2] \cdot (\text{CH}_3\text{OH})_3\}_n$ (**4**), $\{[\text{Cd}(\eta^1\text{-OOCCH}=(\text{CH}_3)\text{CFc})_2(\text{bbbm})] \cdot (\text{CH}_3\text{OH})_2\}_n$ (**5**), and $[\text{Cd}(\eta^2\text{-OOCCH}=(\text{CH}_3)\text{CFc})_2(\text{pmbbm})]_n$ (**6**)

Crystallographic analysis reveals that **4** and **5** both crystallize in the triclinic space group *P*-1 and exhibit 1-D ladder-like structures. As depicted in figure 6(a), each six-coordinate Mn(II) displays a distorted octahedral geometry, provided by two oxygens (O2, O2A) from two $\eta^1\text{-OOCCH}=(\text{CH}_3)\text{CFc}$ groups, two oxygens (O1, O1A) from two waters, and two nitrogens (N1, N1A) from two bbbm ligands. The bond angles around Mn(II) vary from 87.26(13) to 180.00(19)°. The Mn–O lengths are 2.160(3)–2.220(3) Å, and Mn–N lengths are 2.260(3) Å. In **5**, the coordination environment of Cd(II) is consistent with **4**, except the coordinated water is replaced by methanol. The bond angles around Cd(II) vary from 87.64(12)–180.00(12)°. The Cd–O lengths are 2.262(2) and 2.381(2) Å, and Cd–N lengths are 2.325(2) Å. Aromatic rings in **4** and **5** also form π – π stacking interactions for **1**–**3**. figure 6(b) reveals that an infinite 2-D layer of **4** was formed by π – π stacking between two adjacent benzimidazole rings with inter-planar separation of 3.55 Å (center-to-center separation: 4.10 Å). These nearly parallel layers are further assembled by edge-to-face CH/ π interactions of 3.15 Å (dihedral angle: 74.6°, H/ π -plane separation: 2.76 Å) between two adjacent benzimidazole and ferrocene rings to infinite 3-D supramolecular networks. Similarly, the 1-D chains of **5** are extended to 3-D structures by similar π – π stacking interactions for **4**. Intramolecular O···H···O hydrogen bonds are observed in **4** and **5**,

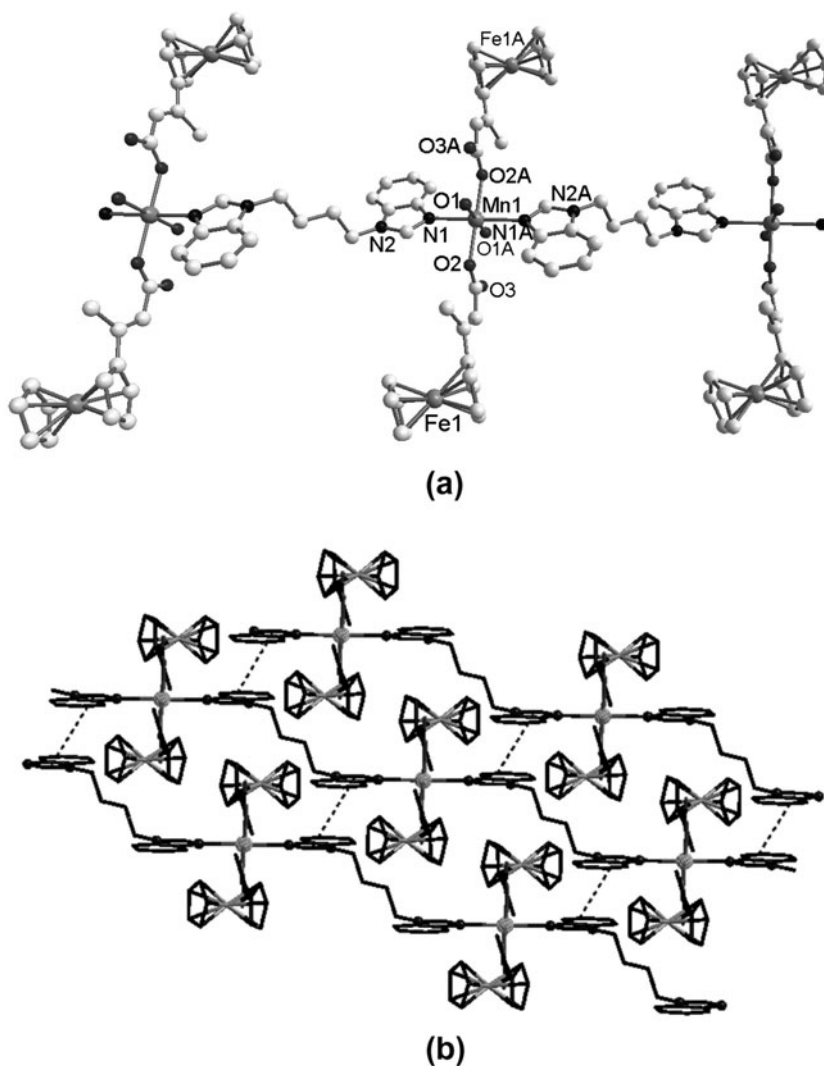


Figure 6. (a) Coordination environment of $\{[\text{Mn}(\eta^1\text{OOCCH}=(\text{CH}_3)\text{CFc})_2(\text{bbbm})(\text{H}_2\text{O})_2]\cdot(\text{CH}_3\text{OH})_3\}_n$ (**4**) with partial atom-labeling scheme. (b) 2-D layered supramolecular network of **4**. The dashed lines represent π - π stacking interactions between two adjacent benzimidazole rings. Hydrogens and solvent molecules are omitted for clarity in (a) and (b).

which stabilize the crystalline solvent at two sides of the molecule chain. The $\text{O}\cdots\text{O}$ distances of the hydrogen bonds are 2.684 Å for **4** and 2.657 Å for **5** and the bond angles around $\text{O}\cdots\text{H}\cdots\text{O}$ are 125.57° for **4** and 169.11° for **5**.

Each $\text{Cd}(\text{II})$ in **6** (figure 7(a)) is six-coordinate by four oxygens (O1, O2, O3, O4) from two η^2 - $\text{OOCCH}=(\text{CH}_3)\text{CFc}$ and two nitrogens (N2, N3) from two pmbbm in a distorted octahedral environment. The $\text{Cd}-\text{N}$ bond lengths are 2.291(3) and 2.308(3) Å, shorter than $\text{Cd}-\text{O}$ lengths [2.311(3)–2.385(3) Å], which are consistent with those of **1**. Similar to **4** and **5**, the 1-D chains of **6** are also extended to a 3-D supramolecular network (figure 7 (b)) by intermolecular π - π stacking interactions between adjacent benzimidazole and

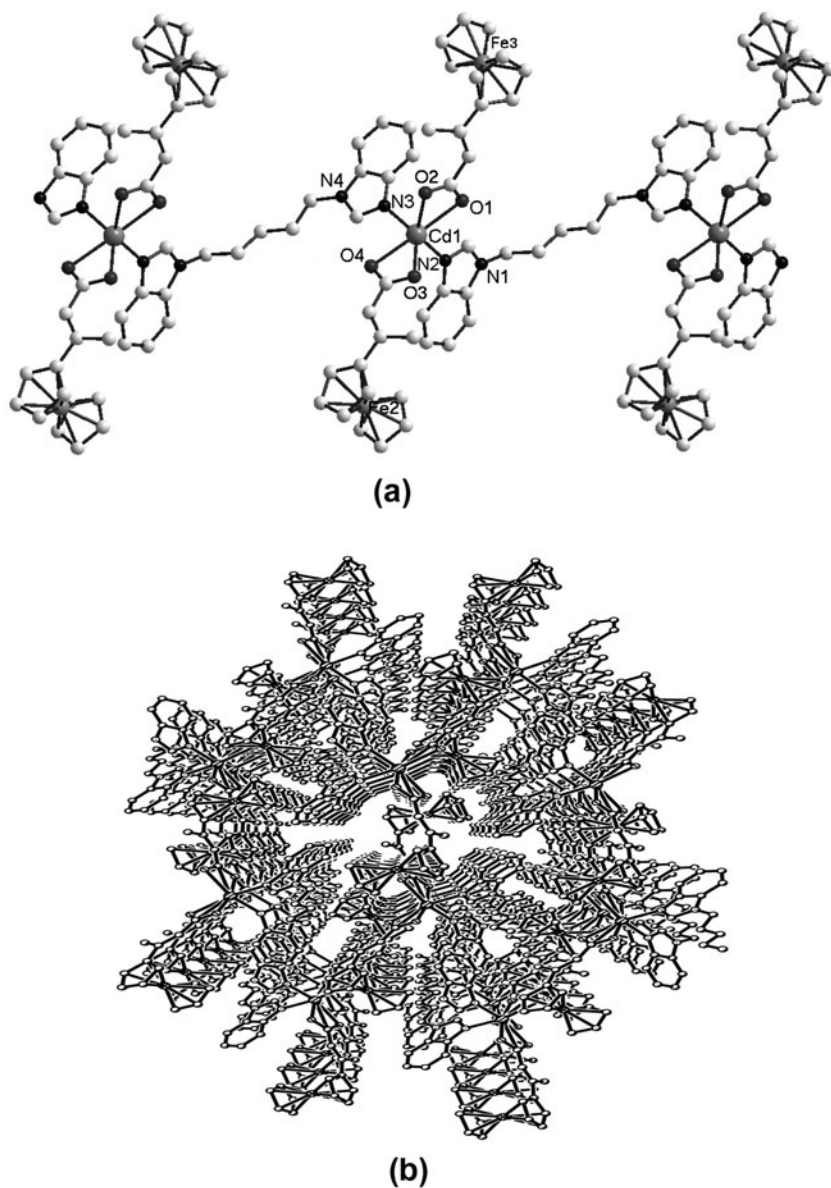


Figure 7. (a) Perspective view of the 1-D chain of $[\text{Cd}(\eta^2\text{-OOCCH}=(\text{CH}_3)\text{CFc})_2(\text{pmbbm})]_n$ (**6**) with partial atom-labeling scheme. (b) 3-D supramolecular network of **6**. Hydrogens are omitted for clarity in figures (a) and (b).

ferrocene rings with inter-planar separation of 3.37 Å (center-to-center separation: 3.76 Å) and edge-to-face CH/ π interactions of 2.75 Å (dihedral angle: 95.0°; H/ π -plane separation: 2.73 Å), respectively. Intramolecular O \cdots H \cdots O hydrogen bonds are observed with O \cdots O distance of 2.727 Å and O \cdots H \cdots O bond angle of 164.83° that further stabilize the crystal structure. These π - π interactions are very important in all six complexes, where they contribute significantly to crystal engineering.

By taking advantage of different bridging nitrogen-heterocyclic ligands, six complexes ranging from binuclear molecular architectures to infinite 1-D polymers were constructed. Comparing the two structural types, ligands with *cis*-conformation tend to form binuclear structures, while ligands with longer flexible chain adopt 1-D geometry. The result is consistent with our previous reports [17, 21, 28–30], in which the differences in bridging ligands and their flexibility have important implications for the structures of crystals. The bridging ligands, therefore, can be used as structure-directing agents to control and tune the crystal structures in a two-ligand assembly process.

3.3. Electrochemical properties of 1–6

Solution-state cyclic voltammetry and differential pulse voltammetry of 1–6 and the 3-ferrocenyl-2-crotonic acid have been studied and are shown in figure 8(a) and (b). Figure 8(a)

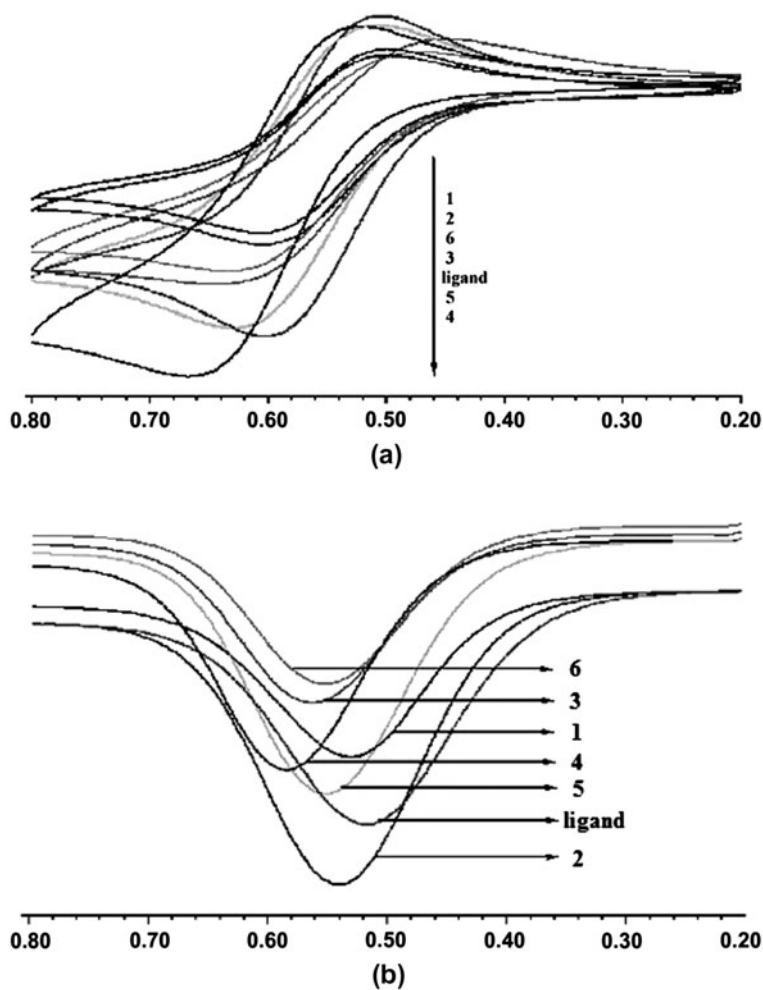


Figure 8. Cyclic voltammograms (a) and differential pulse voltammograms (b) of 1–6 and NaOOCCH=(CH₃)CFc (5.0 × 10⁻⁴ M) in DMF solution containing *n*-Bu₄NClO₄ (0.10 M).

shows that all these complexes exhibit a quasi-reversible redox wave which has been observed in several ferrocene-carboxylate containing complexes [31–33]. In figure 8(b), these complexes show a single peak with a half-wave potential at 0.528 V for **1**, 0.544 V for **2**, 0.564 V for **3**, 0.584 V for **4**, 0.552 V for **5**, 0.556 V for **6**, and 0.516 V for the ligand, which correspond to redox processes of the Fe(II)/Fe(III) couple during electron-transfer in the ferrocenyl moieties [34, 35]. Relative to free HOOCCH=(CH₃)CfC (0.516 V), the half-wave potentials of **1–6** are all shifted to slightly higher potential. The reason is that the electron-withdrawing nature of the coordinated metal centers makes the ferrocene unit harder to oxidize [36, 37]. The half-wave potential of the ferrocenyl moiety in **4** (0.584 V) has a slightly higher value than the other complexes. The possible reason is that Mn(II) has the smallest radius and the strongest electron-withdrawing nature. The result is consistent with our previous literatures [38, 39] where Mn(II)-containing complexes also show the largest shift.

Supplementary material

Crystallographic data for the structures reported in this paper have been deposited with the Cambridge Crystallographic Data Center as supplementary publication with CCDC numbers 868726–868731 (**1**, **2**, **3**, **5**, **6**, **4**). Copies of the data can be obtained free of charge on application to CCDC, 12 Union Road, Cambridge CB2 1EZ, UK (Fax: (44) 1223 336-033; E-mail: deposit@ccdc.cam.ac.uk).

Acknowledgments

We are thankful for financial support from the National Outstanding Young Scholarship (No. 30825043) and National Natural Science Foundation (Nos. 20971110, J0830412, and 91022013), China Postdoctoral Science Foundation (No. 20110491005), Youth Foundation of Shanxi Province (No. 2010021022-1), Program for New Century Excellent Talents of Ministry of Education of China (NCET-07-0765) and the Outstanding Talented Persons Foundation of Henan Province.

References

- [1] P.J. Hagrman, D. Hagrman, J. Zubieta. *Angew. Chem. Int. Ed. Engl.*, **38**, 2638 (1999).
- [2] J.J. Perry, G.J. McManus, M.J. Zaworotko. *Chem. Commun.*, **22**, 2534 (2004).
- [3] M.D. Bartholoma, A.S. Louie, J.F. Valliant, J. Zubieta. *Chem. Rev.*, **110**, 2903 (2010).
- [4] J.P. Li, L.K. Li, H.W. Hou, Y.T. Fan. *Cryst. Growth Des.*, **9**, 4504 (2009).
- [5] B.F. Hoskins, R. Robson. *J. Am. Chem. Soc.*, **112**, 1546 (1990).
- [6] M. Kondo, T. Yoshitomi, K. Seik, H. Matsuzaka, S. Kitagawa. *Angew. Chem. Int. Ed. Engl.*, **36**, 1725 (1997).
- [7] X. Li, B.L. Wu, W. Liu, H.Y. Zhang. *Inorg. Chem. Commun.*, **11**, 1308 (2008).
- [8] J.J. Perry, V.C. Kravtsov, G.J. McManus, M.J. Zaworotko. *J. Am. Chem. Soc.*, **129**, 10076 (2007).
- [9] K. Kobayashi, A. Sato, S. Sakamoto, K. Yamaguchi. *J. Am. Chem. Soc.*, **125**, 3035 (2003).
- [10] W. Ouellette, H.X. Liu, C.J. O'Connor, J. Zubieta. *Inorg. Chem.*, **48**, 4655 (2009).
- [11] E.Q. Gao, S.Q. Bai, Z.M. Wang, C.H. Yan. *J. Am. Chem. Soc.*, **125**, 4984 (2003).
- [12] A. Togni, T. Hayashi. *Ferrocenes: Homogeneous Catalysis Organic Synthesis, Materials Science*, VCH, New York, NY (1995).
- [13] A. Togni, R.L. Haltermann (Eds.). *Metallocenes*, Wiley-VCH, New York, NY (1998).
- [14] A.G. Osborne, M.W.D. Silva, M.B. Hursthouse, K.M.A. Malik, G. Opromolla, P. Zanello. *J. Organomet. Chem.*, **516**, 167 (1996).

- [15] D. Osella, M. Ferrali, P. Zanello, F. Laschi, M. Fontani, C. Nervi, G. Caviglioglio. *Inorg. Chim. Acta*, **306**, 42 (2000).
- [16] R. Altmann, O. Gausset, D. Horn, K. Jurkschat, M. Schurmann, M. Fontani, P. Zanello. *Organometallics*, **19**, 430 (2000).
- [17] J.P. Li, L.K. Li, H.W. Hou, Y.T. Fan. *J. Organomet. Chem.*, **694**, 1359 (2009).
- [18] O.M. Yaghi, C.E. Davis, G.M. Li, H.L. Li. *J. Am. Chem. Soc.*, **119**, 2861 (1997).
- [19] Y.G. Li, N. Hao, Y. Lu, E.B. Wang, Z.H. Kang, C.G. Hu. *Inorg. Chem.*, **42**, 3119 (2003).
- [20] J.P. Li, Y. Hou, X.F. Li, H.J. Lü, H.W. Hou. *Synth. React. Inorg. Met.-Org. Chem.*, **40**, 893 (2010).
- [21] X.J. Shi, X. Wang, L.K. Li, H.W. Hou, Y.T. Fan. *Cryst. Growth Des.*, **10**, 2490 (2010).
- [22] J.P. Li, X.F. Li, H.J. Lü, Y.Y. Zhu, H. Sun, Y.X. Guo, Z.F. Yue, J.A. Zhao, M.S. Tang, H.W. Hou, Y.T. Fan, J.B. Chang. *Inorg. Chim. Acta*, **384**, 163 (2012).
- [23] P. Hu, K.Q. Zhao, L.F. Zhang. *J. Si Chuan Normal Univ. (Nat. Sci. Ed.)*, **21**, 433 (1998).
- [24] X.J. Xie, G.S. Yang, L. Cheng, F. Wang. *Huaxue Shiji (Chin. Ed.)*, **22**, 222 (2000).
- [25] G.M. Sheldrick. *SHELXTL-97, Program for Refining Crystal Structure Refinement*, University of Göttingen, Germany (1997).
- [26] L.K. Li, B.Y. Chen, Y.L. Song, G. Li, H.W. Hou, Y.T. Fan, L.W. Mi. *Inorg. Chim. Acta*, **344**, 95 (2003).
- [27] B. Xiao, H.Y. Han, X.R. Meng, Y.L. Song, Y.T. Fan, H.W. Hou, Y. Zhu. *Inorg. Chem. Commun.*, **7**, 378 (2004).
- [28] X.J. Shi, Q.X. Li, Y.S. Zhang, X.L. Chang, H.W. Hou. *J. Coord. Chem.*, **64**, 3918 (2011).
- [29] H.W. Hou, L.K. Li, G. Li, Y.T. Fan, Y. Zhu. *Inorg. Chem.*, **42**, 3501 (2003).
- [30] J.P. Li, L.K. Li, H.W. Hou, Y.T. Fan, L.H. Gao. *Inorg. Chim. Acta*, **362**, 4671 (2009).
- [31] M.W. Cooke, T.S. Cameron, K.N. Robertson, J.C. Swarts, M.A.S. Aquino. *Organometallics*, **21**, 5962 (2002).
- [32] G. Li, Y.L. Song, H.W. Hou, L.K. Li, Y.T. Fan, Y. Zhu, X.R. Meng, L.W. Mi. *Inorg. Chem.*, **42**, 913 (2003).
- [33] M.W. Cooke, C.A. Murphy, T.S. Cameron, J.C. Swarts, M.A.S. Aquino. *Inorg. Chem. Commun.*, **3**, 721 (2000).
- [34] G.L. Zheng, J.F. Ma, Z.M. Su, L.K. Yan, J.Y. Yang, Y. Li. *Angew. Chem. Int. Ed.*, **4**, 2409 (2004).
- [35] E.M. Barranco, O. Crespo, M.C. Gimeno, P.G. Jones, A. Laguna, C. Sarroca. *J. Chem. Soc., Dalton Trans.*, 2523 (2001).
- [36] L.K. Li, Y.L. Song, H.W. Hou, Y.T. Fan, Y. Zhu. *Eur. J. Inorg. Chem.*, **16**, 3238 (2005).
- [37] R. Horikoshi, T. Mochida, H. Moriyama. *Inorg. Chem.*, **41**, 3017 (2002).
- [38] J.P. Li, Y.L. Song, H.W. Hou, M.S. Tang, Y.T. Fan, Y. Zhu. *J. Organomet. Chem.*, **692**, 1584 (2007).
- [39] H.W. Hou, L.K. Li, Y. Zhu, Y.T. Fan, Y.Q. Qiao. *Inorg. Chem.*, **43**, 4767 (2004).